

Magnetocrystalline anisotropy and Gilbert damping in iron-rich $\text{Fe}_{1-x}\text{Si}_x$ thin films

I. Barsukov,^{1,*} S. Mankovsky,² A. Rubacheva,¹ R. Meckenstock,¹ D. Spoddig,¹ J. Lindner,¹ N. Melnichak,¹ B. Krumme,¹ S. I. Makarov,¹ H. Wende,¹ H. Ebert,² and M. Farle¹

¹Fakultät für Physik and Center for Nanointegration Duisburg-Essen (CeNIDE), Universität Duisburg-Essen, D-47048 Duisburg, Germany

²Department of Chemistry/Phys. Chemistry, LMU Munich, Butenandtstrasse 11, D-81377 Munich, Germany

(Received 21 July 2011; revised manuscript received 7 September 2011; published 8 November 2011)

The magnetocrystalline anisotropy of $\text{Fe}_{1-x}\text{Si}_x$ ($0 \leq x \leq 0.4$) epitaxial thin films on $\text{MgO}(001)$ was studied by ferromagnetic resonance. The experimental results are in good agreement with theoretical predictions of *ab initio* electronic structure calculations using the fully relativistic Korringa-Kohn-Rostoker Green's function method within spin-density-functional theory. The Gilbert damping α is found to be isotropic by theory and experiment with a minimum at the composition $x = 0.2$.

DOI: [10.1103/PhysRevB.84.180405](https://doi.org/10.1103/PhysRevB.84.180405)

PACS number(s): 75.30.Gw, 76.60.Es, 31.15.A-

For many years Fe-Si alloys in the Fe-rich regime have been considered to be materials having attractive technical characteristics. These alloys have reduced magnetic anisotropy and increased resistivity when compared to pure Fe, making them interesting materials for technical applications.¹⁻⁴ In particular, special attention has been attributed to the binary Heusler alloy $\text{Fe}_{0.75}\text{Si}_{0.25}$ due to its half-metallic ferromagnetic features and high Curie temperature. The magnetization relaxation of $\text{Fe}_{0.75}\text{Si}_{0.25}/\text{MgO}(001)$ thin films has been studied recently.^{5,6} The authors in Refs. 6 and 7 identified extrinsic and intrinsic spin relaxation channels which were quantitatively modeled using the theoretical framework of Arias and Mills.⁸ Fe-rich $\text{Fe}_{0.945}\text{Si}_{0.055}/\text{MgO}(001)$ films were found to exhibit pure Gilbert damping⁵ in contrast to $\text{Fe}_{0.75}\text{Si}_{0.25}/\text{MgO}(001)$. In the latter, spin dynamics could be tailored, inducing a uniaxial two-magnon scattering channel by oblique deposition of Si.⁶ To better understand the role of magnetocrystalline anisotropy (MCA) and intrinsic spin relaxation for the manipulation of magnetization dynamics, we present here a combined experimental and theoretical work, focusing on nearly strain-free monocrystalline $\text{Fe}_{1-x}\text{Si}_x$ alloys.

To describe the Gilbert damping in magnetic systems theoretically, various models have been used in the past. The best microscopic understanding of spin relaxation in a specific system, however, can be obtained on the basis of *ab initio* electronic structure calculations. In the past the most detailed *ab initio* calculations of Gilbert damping in metallic systems have been done either within the so-called breathing Fermi-surface model by Kambersky *et al.*⁹ and Fähnle *et al.*¹⁰⁻¹² or within the more general torque-correlation model by Kambersky¹³ and Gilmore *et al.*¹⁴ Note, however, that the final expressions for the Gilbert damping parameter used in these calculations still include a phenomenological relaxation time τ . In contrast to this, Brataas *et al.*¹⁵ worked out a method for calculating the Gilbert damping in terms of a scattering matrix S . This approach accounts for all scattering processes at $T = 0$ K and gives rather good agreement with the experimental results for disordered transition-metal alloys, as was demonstrated recently by Starikov *et al.*¹⁶

A very efficient implementation of this linear response formalism for calculations of the Gilbert damping parameters was worked out by us recently, adapting the ideas of Brataas *et al.*¹⁵ and making use of the advantages of the Korringa-Kohn-Rostoker (KKR) Green's function method based on

multiple-scattering theory.¹⁷ In particular, in combination with the coherent potential approximation (CPA), spin relaxation in disordered systems can be calculated. Our present approach accounts for all scattering processes at $T = 0$ K in Gilbert damping calculations.

Epitaxial $\text{Fe}_{1-x}\text{Si}_x$ thin films ($0 \leq x \leq 0.4$) in the thickness range of 10–40 nm were grown by molecular beam epitaxy on $\text{MgO}(001)$ substrates or on a several-nanometer-thick MgO tunneling barrier on $\text{GaAs}(001)$. Fe and Si were simultaneously codeposited at 250 °C. The nominal Fe-deposition rate was held at less than 1 Å/s while retaining a pressure of 1×10^{-9} mbar. The films were protected against oxidation by a capping layer of Cr or MgO . Similar to pure Fe on $\text{MgO}(001)$, these Fe-Si films are cubic systems growing crystallographically rotated by 45° with respect to the $\text{MgO}(001)$ axes ($(100)_{\text{Fe-Si}} \parallel (110)_{\text{MgO}}$) in the film plane.

Static and dynamic magnetic parameters were studied by ferromagnetic resonance (FMR).^{7,18-20} For angular-dependent measurements a cylindrical microwave cavity with a TE_{110} mode at 9.8 GHz was used. The resonance fields measured at room temperature were fitted (Fig. 1) using the Smit-Beljers approach²⁰

$$\left(\frac{\omega}{\mu_B g / \hbar}\right)^2 = \frac{1}{M^2 \sin^2(\theta)} \left[\frac{\partial^2 F}{\partial \theta^2} \frac{\partial^2 F}{\partial \phi^2} - \left(\frac{\partial^2 F}{\partial \theta \partial \phi}\right)^2 \right], \quad (1)$$

where ω is the microwave frequency, g is the g factor, and ϕ and θ are the azimuthal and polar equilibrium angles of the vector of magnetization M .

The following expression for the free-energy density functional F was used:²⁰

$$F = -\vec{M} \cdot \vec{B}_{\text{ext}} - M B_{\perp} \cos^2 \theta + K_2^{\parallel} \sin^2 \theta \sin^2(\phi - \phi_{K_2}) + K_4 \sin^2 \theta - \frac{K_4}{8} (7 + \cos 4\phi) \sin^4 \theta, \quad (2)$$

which includes the Zeeman term, the perpendicular anisotropy field B_{\perp} , the in-plane uniaxial anisotropy K_2^{\parallel} with its easy axis ϕ_{K_2} , and the cubic magnetocrystalline anisotropy (MCA) K_4 . The anisotropy fields K_i/M can be obtained with an accuracy of <1%. The error of the anisotropy constants is dominated by the uncertainty of the saturation magnetization of $\leq 10\%$, evaluated from superconducting quantum interference device (SQUID) measurements. The uniaxial anisotropy K_2^{\parallel} is

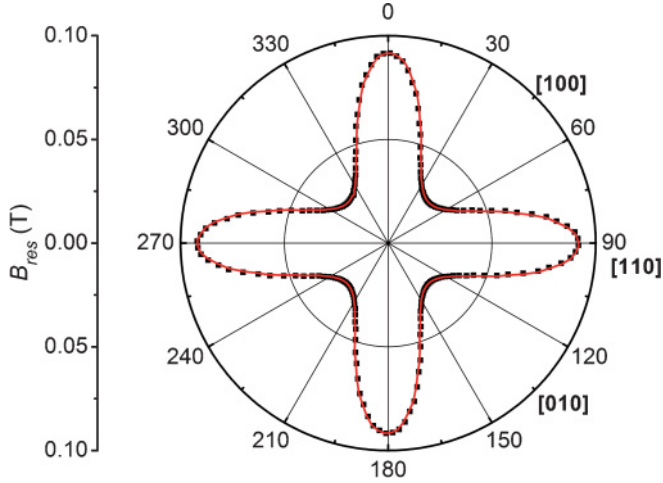


FIG. 1. (Color online) Polar plot of the resonance fields of the sample with 10% Si at room temperature at 9.8 GHz as a function of the in-plane angle of the external field. Black dots: Experimental data with error bar smaller than the symbol size. Red (gray) line: Fit according to Eqs. (1) and (2).

negligibly small in all samples, and the cubic MCA constant K_4 monotonously decreases with an increasing concentration of Si, as shown in Fig. 2(a).

For the films with 5.5%, 25%, and 35% Si, additional measurements at higher frequencies in the k -band and Q -band regimes were performed in order to extract dynamic magnetic parameters. For separating intrinsic and extrinsic spin relaxation processes, in-plane angular-dependent and frequency-dependent data, accompanied with calculations of the magnetic high-frequency susceptibility, were processed as explained in Refs. 5 and 7. The Gilbert damping has been found to be *isotropic*, and the values of the Gilbert parameter α are shown in Fig. 2(b).

Ab initio electronic structure calculations have been performed for bulk systems using the fully relativistic KKR method²¹ within density functional theory (DFT). The exchange-correlation potential is constructed within the local spin-density approximation (LSDA) using the parametrization of Vosko, Wilk, and Nusair.²² For the angular momentum expansion of the Green's function, a cutoff of $l_{\max} = 3$ is applied. For the integrations over the Brillouin zone (BZ) we used a regular k mesh with $\sim 1.5 \times 10^6$ k points for the self-consistent field (SCF) and magnetic torque calculations, and $\sim 5 \times 10^6$ k points for Gilbert damping calculations.

The investigation of the MCA is based on calculations of the magnetic torque \vec{T} acting on the magnetic moment \vec{M} aligned along the direction \vec{e}_M .²³ Here we used the component of the magnetic torque along the direction \vec{u} within the plane perpendicular to the z axis and orthogonal to the direction of the magnetic moment \vec{e}_M . It is characterized by the angles θ and ϕ describing the \vec{e}_M direction, i.e., one has $T_{\vec{u}}(\theta, \phi) = -\partial E[M(\theta, \phi)]/\partial \theta$.

The MCA constants K_4 were determined by mapping the *ab initio* torque results onto the model expression $E_{\text{model}} = K_4 V(\alpha_x^2 \alpha_y^2 + \alpha_y^2 \alpha_z^2 + \alpha_z^2 \alpha_x^2)$ and are shown in Fig. 2(a). It should be stressed that calculating the MCA constant K_4 via the magnetic torque enhances substantially the numerical

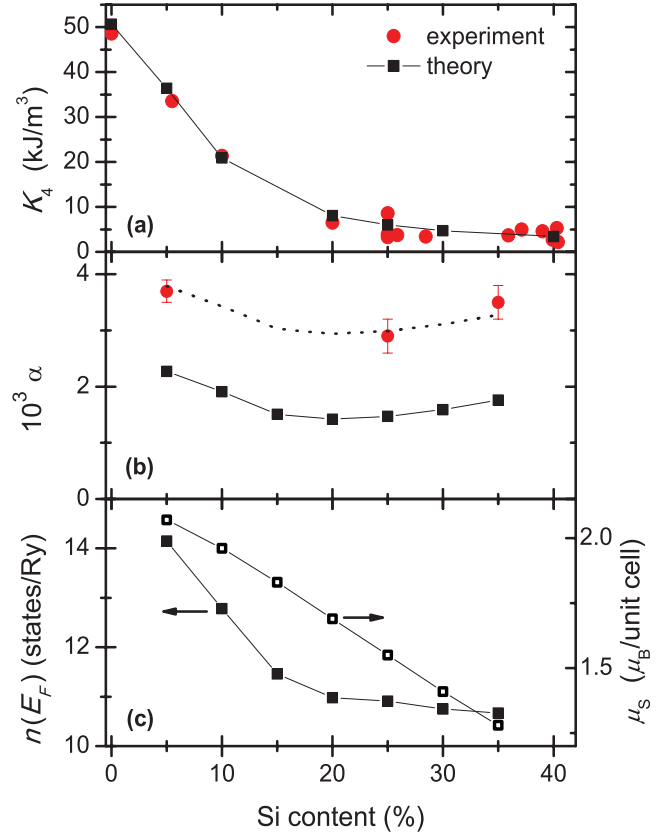


FIG. 2. (Color online) (a) Cubic MCA constant K_4 as a function of the Si concentration in $\text{Fe}_{1-x}\text{Si}_x$. Red (gray) dots: Experimental data (error bar $\leq 10\%$, uncertainty of Si content $< 1\%$) obtained from FMR on thin films at room temperature. Black squares: Theoretical data from *ab initio* DFT calculations. Experimental data for $x = 0$ are taken from Ref. 28. (b) Gilbert parameter α . The dashed line represents the theoretical data shifted by an offset of $+1.5 \times 10^{-3}$. (c) Density of states $n(E_F)$ at the Fermi level and the average spin magnetic moment μ_S .

stability of the calculations compared to calculations via the total energy or using the force theorem.²⁴ Performing the necessary energy integration in the complex energy plane furthermore reduces the numerical effort for the k -space integrals.

While the experimental results have been obtained at room temperature, the calculations correspond to $T = 0$ K, i.e., all the temperature effects have been neglected both in Gilbert damping as well as in the MCA. The effect of the tetragonal distortion in the films is assumed to be small²⁵ in the thickness range studied here, and therefore is not taken into account in the calculations.

The calculations of the diagonal elements α_{xx} and α_{yy} of the Gilbert damping tensor for the $\text{Fe}_{0.95}\text{Si}_{0.05}$ alloy have been performed first within the atomic sphere approximation (ASA). Two different directions of the magnetization, [001] and [011], have been considered, which correspond to two possible crystallographic orientations in the film plane. The Gilbert damping tensor elements were found to be $\alpha_{xx} = \alpha_{yy} = 0.00123$ for [001], and $\alpha_{xx} = 0.00123$ and $\alpha_{yy} = 0.00127$ for [011] magnetization directions, i.e., they are basically isotropic. Thus, in the following, we discuss the Gilbert

damping parameter as a scalar instead of tensorial quantity. Further calculations were done for the [001] direction in the full potential mode. In this case we obtained $\alpha = 0.00227$, which is in much better agreement with the experimental value $\alpha = 0.0037(2)$. The results for other Si concentrations are shown in Fig. 2(b). The difference between the theoretical and experimental values of α seems to be *constant* over the entire Si content range [Fig. 2(b)] and can be attributed to the following: (i) Although the magnetization damping due to two-magnon scattering processes is taken into account when evaluating the Gilbert parameter, some other damping mechanisms still can be present, e.g., those related to the finite film thickness²⁶ and which are not accounted for in the bulk calculations.²⁷ (ii) The measurements were performed at room temperature. This implies additional scattering processes due to thermally excited phonons, which are neglected in the calculations, accounting only for scattering events due to the chemical disorder in the alloy system. Our theoretical results on the temperature dependence of the Gilbert damping in ferromagnetic 3d-transition metals seem to support this explanation. For an experimental proof temperature- and frequency-dependent FMR measurements would be necessary.

An increase of the Si concentration in the alloy leads to a decrease of the Gilbert damping in the region of small Si concentration and to the minimum at $\sim 20\%$ Si [see Fig. 2(b)]. This behavior primarily is a consequence of the increase of content of Si with a small induced magnetic moment, resulting in a decrease of the average magnetic moment, and having a rather small spin-orbit coupling (SOC) strength ξ for *p* and *d* electrons compared to Fe [$\xi_p^{\text{Fe}}(E_F) \approx 0.16$ eV, $\xi_d^{\text{Fe}}(E_F) \approx 0.065$ eV, $\xi_p^{\text{Si}}(E_F) \approx 0.04$ eV, $\xi_d^{\text{Si}}(E_F) \approx 0.0005$ eV]. The variation of the electronic structure with composition also has a pronounced impact that can be seen from the correlation of α with the density of states at the Fermi energy E_F [Fig. 2(c)]. The minimum at $\sim 20\%$ Si can be understood as a result of competition (see Ref. 17) of electronic structure [$n(E_F)$] and total magnetic moment as functions of Si concentration, shown in Fig. 2(c).

The cubic MCA constant K_4 as a function of Si concentration is presented in Fig. 2(a), where the theoretical results are compared with the experimental data. Both results are in good agreement with each other and show a monotonous decrease of K_4 upon an increase of Si content. This behavior is mainly governed by the effects mentioned above in connection with the Gilbert damping. One reason is related to the SOC of Si atoms which is much smaller compared to the SOC of Fe. When the MCA of an alloy is determined by SOC of its components, an increase of Si content should result in a decrease of the MCA. Very important for the MCA, as well as for the Gilbert damping, is the modification of the electronic structure of Fe-Si alloys upon variation of the Si content. As one can see in Fig. 3, the variation of the Si concentration results in two pronounced effects: a shift of the electronic energy bands and their smearing when the amount of Si atoms in the alloy increases. Both effects have a strong influence on the MCA, as well as on the Gilbert damping, if states close to the E_F are involved. As shown in Fig. 3, this indeed takes place in the case of the $\text{Fe}_{0.75}\text{Si}_{0.25}$ alloy for which some of the Fe *d* states move away from the Fermi level when compared to their positions in pure Fe. Note here

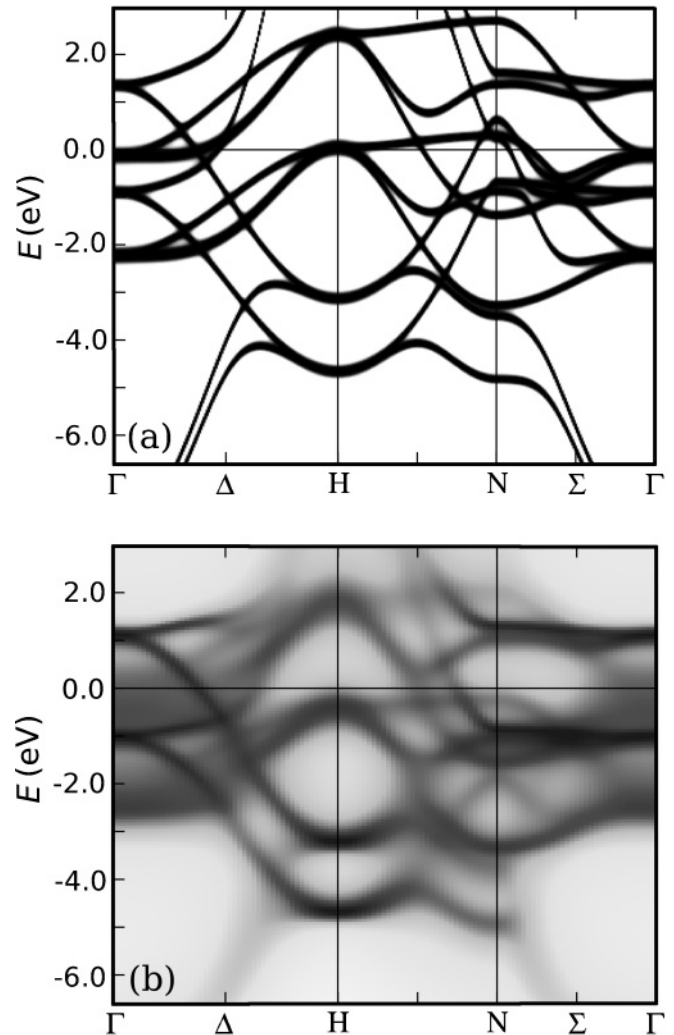


FIG. 3. Bloch spectral function for pure Fe [calculated for an imaginary part of the energy $\text{Im}(E) = 10^{-5}$ Ry] (a) and for the random alloy $\text{Fe}_{0.75}\text{Si}_{0.25}$ (b).

also that the theoretical data correspond to $T = 0$ K while the experimental results are obtained at room temperature. A rather small temperature effect is presumably due to significant smearing of the energy bands [Fig. 3(b)] caused by the chemical disorder in the alloy. The corresponding energy-band modifications due to thermally induced atom displacements as well as spin deviations are much smaller at room temperature and do not essentially influence the MCA. Nevertheless, in the Fe-rich limit the MCA constant measured in the experiment at room temperature is expected to be reduced by $\sim 10\%$.^{28,29} When Si concentration further increases [right-hand side of Fig. 2(b)], the measured MCA shows a dispersion of values for the set of samples used in the experiment, which is larger than the expected temperature effects. Therefore, the temperature properties in this concentration region are not discussed.

In conclusion, we compare *ab initio* calculations and experimental results for the magnetocrystalline anisotropy and Gilbert damping in $\text{Fe}_{1-x}\text{Si}_x$ alloys. The small spin-orbit coupling of Si and the considerable modification of the electronic structure of the alloys upon an increase of Si

content lead to a decrease of the MCA constant and to a nonmonotonous behavior of the Gilbert damping parameter with a minimum at 20% Si. The Gilbert damping has been found to be isotropic, both by the *ab initio* calculations and by the experiment. The theoretical value of the spin relaxation is of the same order of magnitude as the experimental value,

and their difference suggests a significant contribution of spin-phonon scattering processes in the real samples.

We thank U. von Hörsten for preparing the samples. Financial support by the DFG within SFB491 and SFB689 is acknowledged. I.B. thanks Z. Frait for fruitful discussions.

*igor.barsukov@uni-due.de

- ¹B. Viala, J. Degauque, M. Fagot, M. Baricco, E. Ferrara, and F. Fiorillo, *Mater. Sci. Eng. A* **212**, 62 (1997).
- ²J. Kudrnovský, N. E. Christensen, and O. K. Andersen, *Phys. Rev. B* **43**, 5924 (1991).
- ³J. E. Mattson, Sudha Kumar, Eric E. Fullerton, S. R. Lee, C. H. Sowers, M. Grimsditch, S. D. Bader, and F. T. Parker, *Phys. Rev. Lett.* **71**, 185 (1993).
- ⁴A. Kawaharazuka, M. Ramsteiner, J. Herfort, H.-P. Schönherr, H. Kostial, and K. H. Ploog, *Appl. Phys. Lett.* **85**, 3492 (2004).
- ⁵I. Barsukov, R. Meckenstock, J. Lindner, M. Möller, C. Hassel, O. Posth, M. Farle, and H. Wende, *IEEE Trans. Magn.* **46**, 2252 (2010).
- ⁶I. Barsukov, P. Landeros, R. Meckenstock, J. Lindner, B. Krumme, H. Wende, D. L. Mills, and M. Farle (unpublished).
- ⁷Kh. Zakeri, J. Lindner, I. Barsukov, R. Meckenstock, M. Farle, U. von Hörsten, H. Wende, W. Keune, J. Rucker, S. S. Kalarickal, K. Lenz, W. Kuch, K. Baberschke, and Z. Frait, *Phys. Rev. B* **76**, 104416 (2007).
- ⁸R. Arias and D. L. Mills, *Phys. Rev. B* **60**, 7395 (1999).
- ⁹J. Kuneš and V. Kambersky, *Phys. Rev. B* **65**, 212411 (2002).
- ¹⁰M. Fähnle and D. Steiauf, *Phys. Rev. B* **73**, 184427 (2006).
- ¹¹D. Steiauf, J. Seib, and M. Fähnle, *Phys. Rev. B* **78**, 020410 (2008).
- ¹²M. Fähnle, D. Steiauf, and J. Seib, *J. Phys. D* **41**, 164014 (2008).
- ¹³V. Kambersky, *Phys. Rev. B* **76**, 134416 (2007).
- ¹⁴K. Gilmore, Y. U. Idzerda, and M. D. Stiles, *Phys. Rev. Lett.* **99**, 027204 (2007).
- ¹⁵A. Brataas, Y. Tserkovnyak, and G. E. W. Bauer, *Phys. Rev. Lett.* **101**, 037207 (2008).
- ¹⁶A. A. Starikov, P. J. Kelly, A. Brataas, Y. Tserkovnyak, and G. E. W. Bauer, *Phys. Rev. Lett.* **105**, 236601 (2010).
- ¹⁷H. Ebert, S. Mankovsky, D. Ködderitzsch, and P. J. Kelly, *Phys. Rev. Lett.* **107**, 066603 (2011).
- ¹⁸Nan Mo, J. Hohlfield, M. ul Islam, C. S. Brown, E. Girt, P. Krivosik, Wei Tong, A. Rebei, and C. E. Patton, *Appl. Phys. Lett.* **92**, 022506 (2008).
- ¹⁹J. Lindner, K. Lenz, E. Kosubek, K. Baberschke, D. Spoddig, R. Meckenstock, J. Pelzl, Z. Frait, and D. L. Mills, *J. Magn. Magn. Mater.* **272-276** (Suppl. 1), E1653 (2004).
- ²⁰M. Farle, *Rep. Prog. Phys.* **61**, 755 (1998).
- ²¹H. Ebert, in *Electronic Structure and Physical Properties of Solids*, edited by H. Dreyssé, Lecture Notes in Physics Vol. 535 (Springer, Berlin, 2000), p. 191.
- ²²S. H. Vosko, L. Wilk, and M. Nusair, *Can. J. Phys.* **58**, 1200 (1980).
- ²³J. B. Staunton, L. Szunyogh, A. Buruzs, B. L. Gyorffy, S. Ostanin, and L. Udvardi, *Phys. Rev. B* **74**, 144411 (2006).
- ²⁴M. D. Stiles, S. V. Halilov, R. A. Hyman, and A. Zangwill, *Phys. Rev. B* **64**, 104430 (2001).
- ²⁵Y. N. Zhang, J. X. Cao, I. Barsukov, J. Lindner, B. Krumme, H. Wende, and R. Q. Wu, *Phys. Rev. B* **81**, 144418 (2010).
- ²⁶P. J. Jensen, K. H. Bennemann, P. Pouloupoulos, M. Farle, F. Wilhelm, and K. Baberschke, *Phys. Rev. B* **60**, R14994 (1999).
- ²⁷C. Vittoria, S. D. Yoon, and A. Widom, *Phys. Rev. B* **81**, 014412 (2010).
- ²⁸Z. Frait (unpublished) and similar in R. M. Bozorth, *J. Appl. Phys.* **8**, 575 (1937).
- ²⁹Richard M. Bozorth, *Ferromagnetism* (IEEE, New York, 1993).